Electronic Supplementary Material (ESI) for Dalton Transactions.
This journal is © The Royal Society of Chemistry 2018

Electronic Supporting Information (ESI)

Hydrazone-Based Covalent Organic Frameworks for Lewis Acid Catalysis

Tanay Kundu, Jian Wang, Youdong Cheng, Yonghua Du, Yuhong Qian, Guoliang Liu, and Dan Zhao*

Table of Contents

S1: Synthesis of ligands; NMR, mass and IR spectroscopy

Synthesis of diethyl 2,5-dihydroxyterephthalate: In a 500 mL round-bottom-flask, a solution of 2,5-dihydroxyterephthalic acid (5.0 g, 25 mM) in 200 mL of ethanol was mixed with 12 mL of concentrated H_2SO_4. After this, the solution was refluxed overnight and then cooled to precipitate the crude product as white crystalline flakes. The mixture was filtered and the precipitate was recrystallized from ethanol twice and further dried for 24 h at 50 °C to afford the desired compound as a light yellow powder (5.5 g, 70% yield).

Synthesis of 2,5-dihydroxyterephthalohydrazide (2,5-DHTH): In a 500 mL round-bottom-flask, a solution of diethyl 2,5-dihydroxyterephthalate (5.0 g, 19 mM) in 100 mL of ethanol was mixed with 25 mL of hydrazine hydrate (98%, Sigma Aldrich). After refluxing the solution overnight, a pale yellow precipitate appeared. The crude product was filtered and recrystallized from ethanol twice and further dried for 24 h at 50 °C to afford the desired compound as a pale yellow powder (2.5 g, 50% yield).

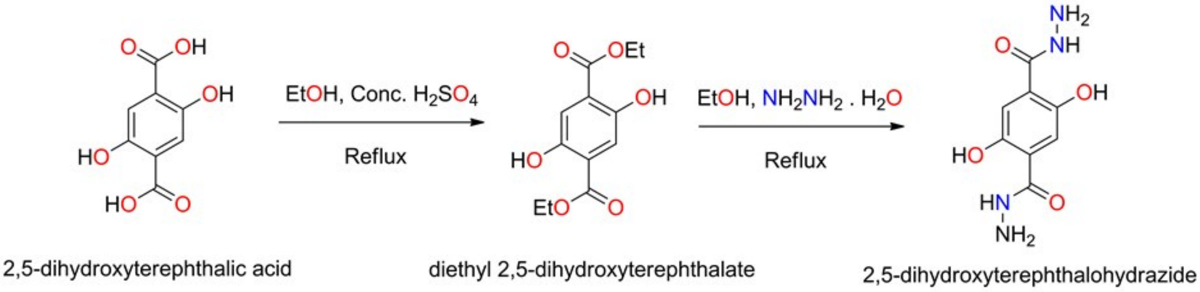

Figure S1. Synthetic scheme of 2,5-DHTH.

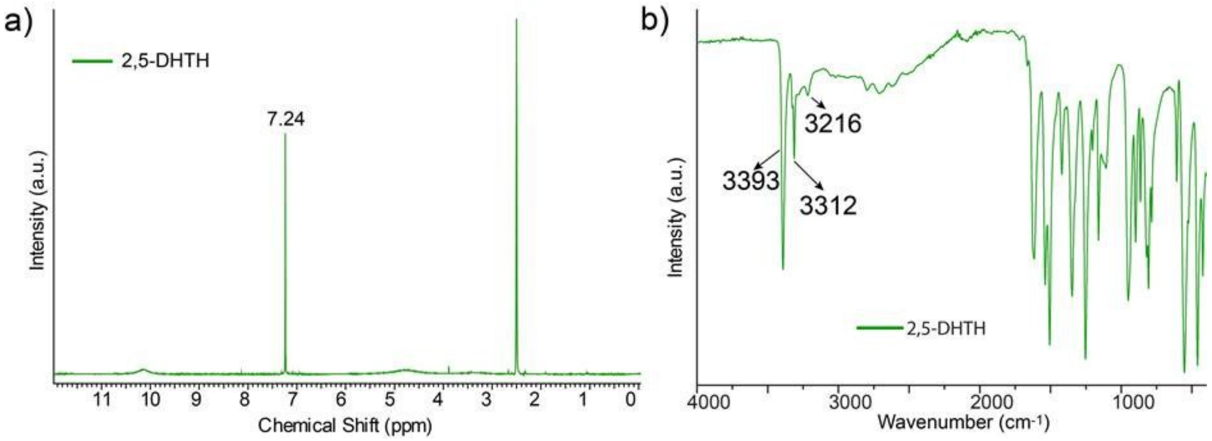

Figure S2. ^{1}H-NMR a) and FT-IR b) spectra of 2,5-DHTH.

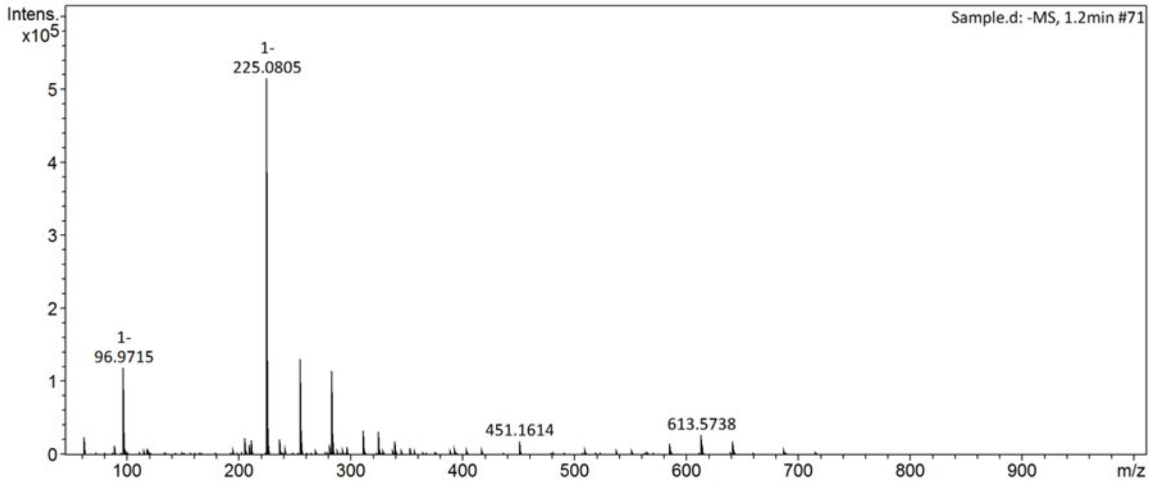

Figure S3. Mass spectrum of 2,5-DHTH.

Synthesis of diethyl 2,3-dihydroxyterephthalate: In a 500 mL round-bottom-flask, a solution of 2,3-dihydroxyterephthalic acid (5.0 g, 25 mM) in 200 mL of ethanol was mixed with 12 mL of concentrated H_2SO_4. After this, the solution was refluxed overnight and then cooled to precipitate the crude product as white crystalline flakes. The mixture was filtered and the precipitate was recrystallized from ethanol twice and further dried for 24 h at 50 °C to afford the desired compound as a grey powder (5.5 g, 70% yield).

Synthesis of 2,3-dihydroxyterephthalohydrazide (2,3-DHTH): In a 500 mL round-bottom-flask, a solution of diethyl 2,3-dihydroxyterephthalate (5.0 g, 19 mM) in 100 mL of ethanol was mixed with 25 mL of hydrazine hydrate (98%, Sigma Aldrich). After refluxing the solution overnight, a pale yellow precipitate appeared. The crude product was filtered and recrystallized from ethanol twice and further dried for 24 h at 50 °C to afford the desired compound as a grey powder (2.0 g, 40% yield).

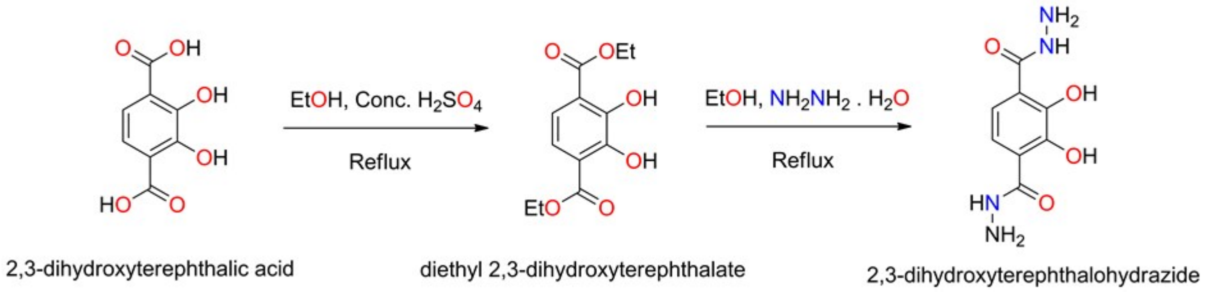

Figure S4. Synthetic scheme of 2,3-DHTH.

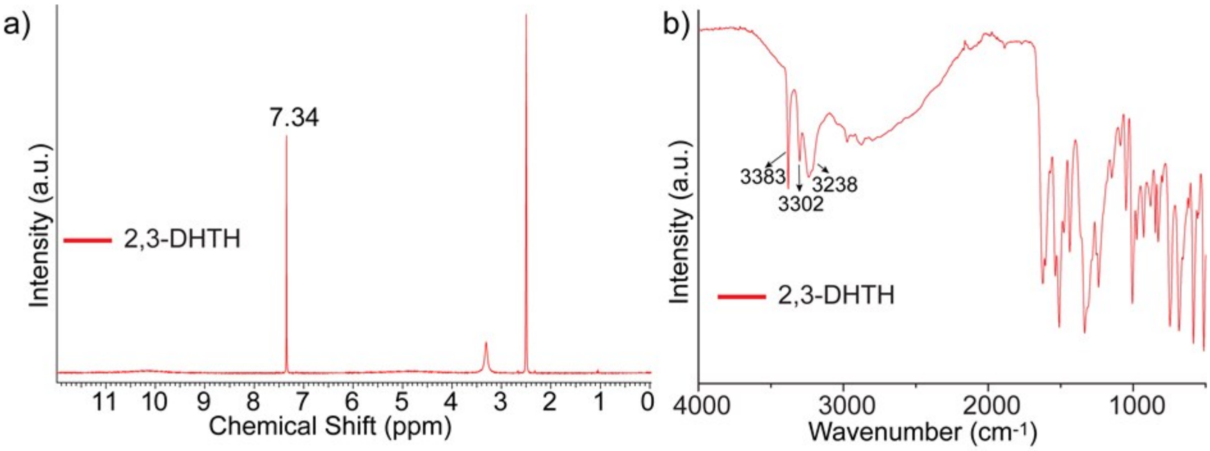

Figure S5. ^{1}H-NMR a) and FT-IR b) spectra of 2,3-DHTH.

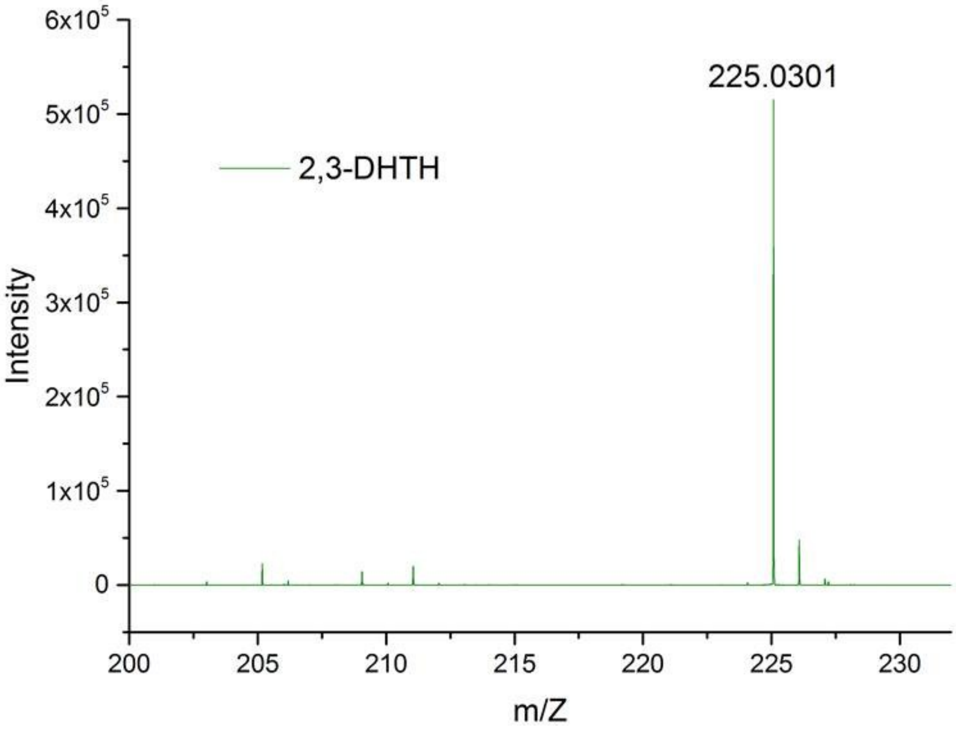

Figure S6. Mass spectrum of 2,3-DHTH.

S2: Synthesis and characterization of reference compounds

Synthesis of Sd-2,5-DHTH: The reference compound for NUS-50 was synthesized as follows. 2,5-DHTH (1 g, 4.4 mM) was dispersed in ethanol, added with salicylaldehyde (2 mL, 16.3 mM) and refluxed overnight. The solution was then filtered and the precipitate was washed with ethanol 2 times. The compound was dried in a vacuum oven at 60 °C for 24 h to obtain a dark yellow powder.

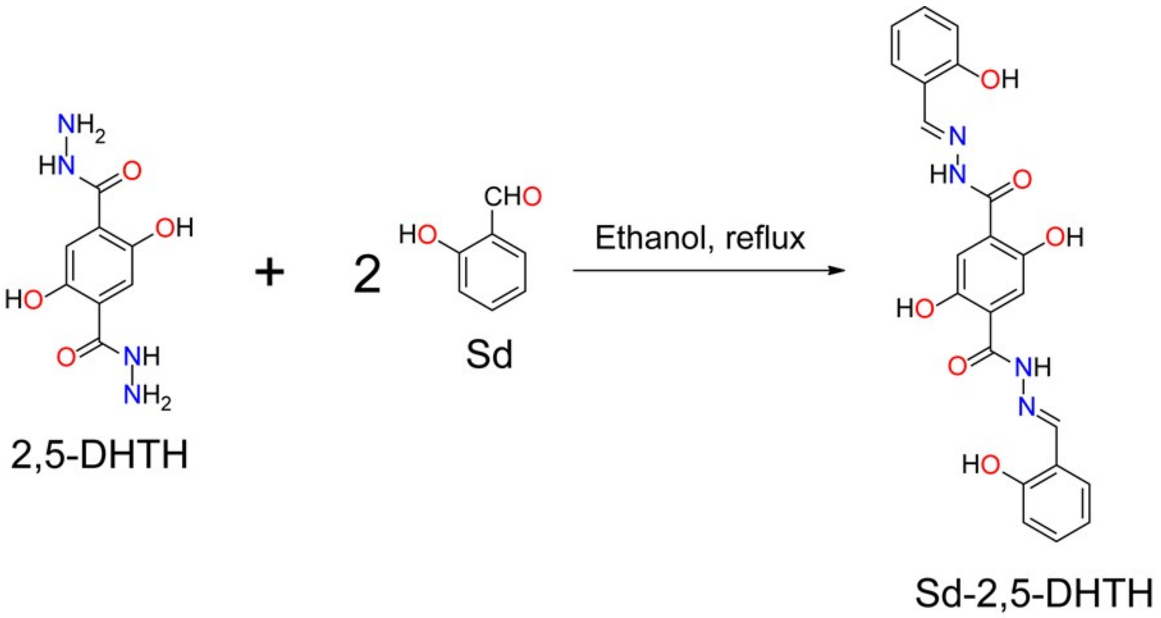

Figure S7. Synthetic scheme of Sd-2,5-DHTH.

Synthesis of Sd-2,3-DHTH: The reference compound for NUS-51 was synthesized as follows. 2,3-DHTH (1 g, 4.4 mM) was dispersed in ethanol, added with salicylaldehyde (2 mL, 16.4 mM) and refluxed overnight. The solution was then filtered and the precipitate was washed with ethanol 2 times. The compound was dried in a vacuum oven at 60 °C for 24 h to obtain a dull yellow powder.

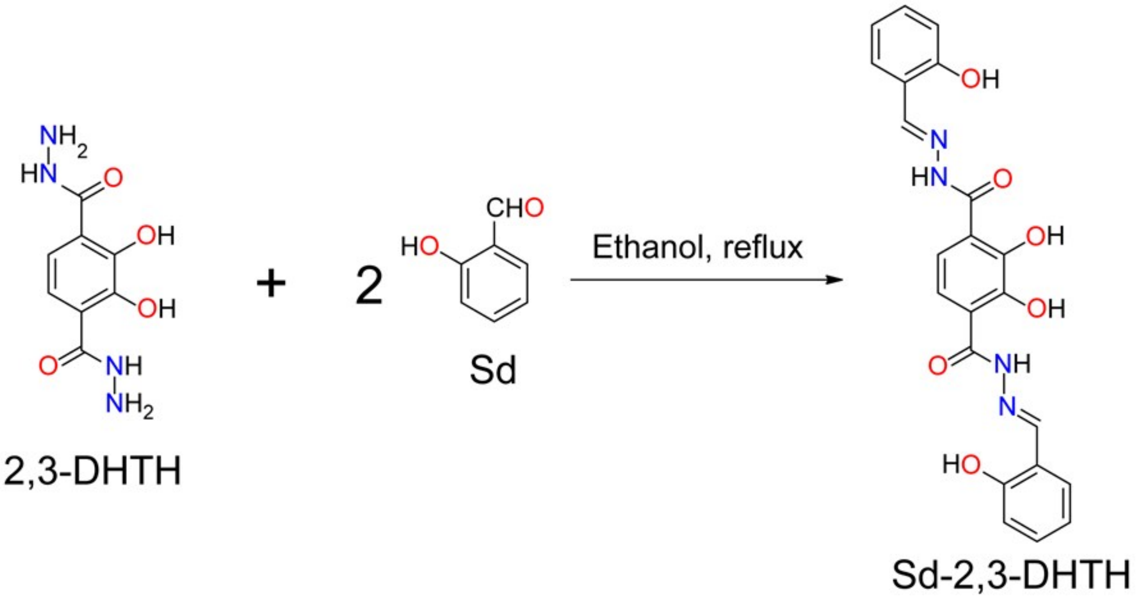

Figure S8. Synthetic scheme of Sd-2,3-DHTH.

Single crystal X-ray diffraction study and crystal structure of Sd-2,3-DHTH: Sd-2,3-DHTH was dissolved in a minimum amount of N,N'-dimethylformamide by heating and kept aside for methanol diffusion overnight in a closed glass vial. The crystals were harvested after 3 days, collected by filtration and subjected to single crystal X-ray diffraction measurement. The as-synthesized crystal of Sd-2,3-DHTH was taken out from the mother solution, coated with paratone-N, placed on top of a nylon cryoloop (Hampton research) and then mounted in the Bruker SMART APEX single crystal X-ray diffractometer. The data collection was done at 100 K. The data can be retrieved from CCDC using the number 1586508. The ellipsoids in ORTEP diagram is displayed at the 50% probability level.[1] Despite numerous attempts, Sd-2,5-DHTH could not be crystallized in a similar fashion, yielding only microcrystalline powder.

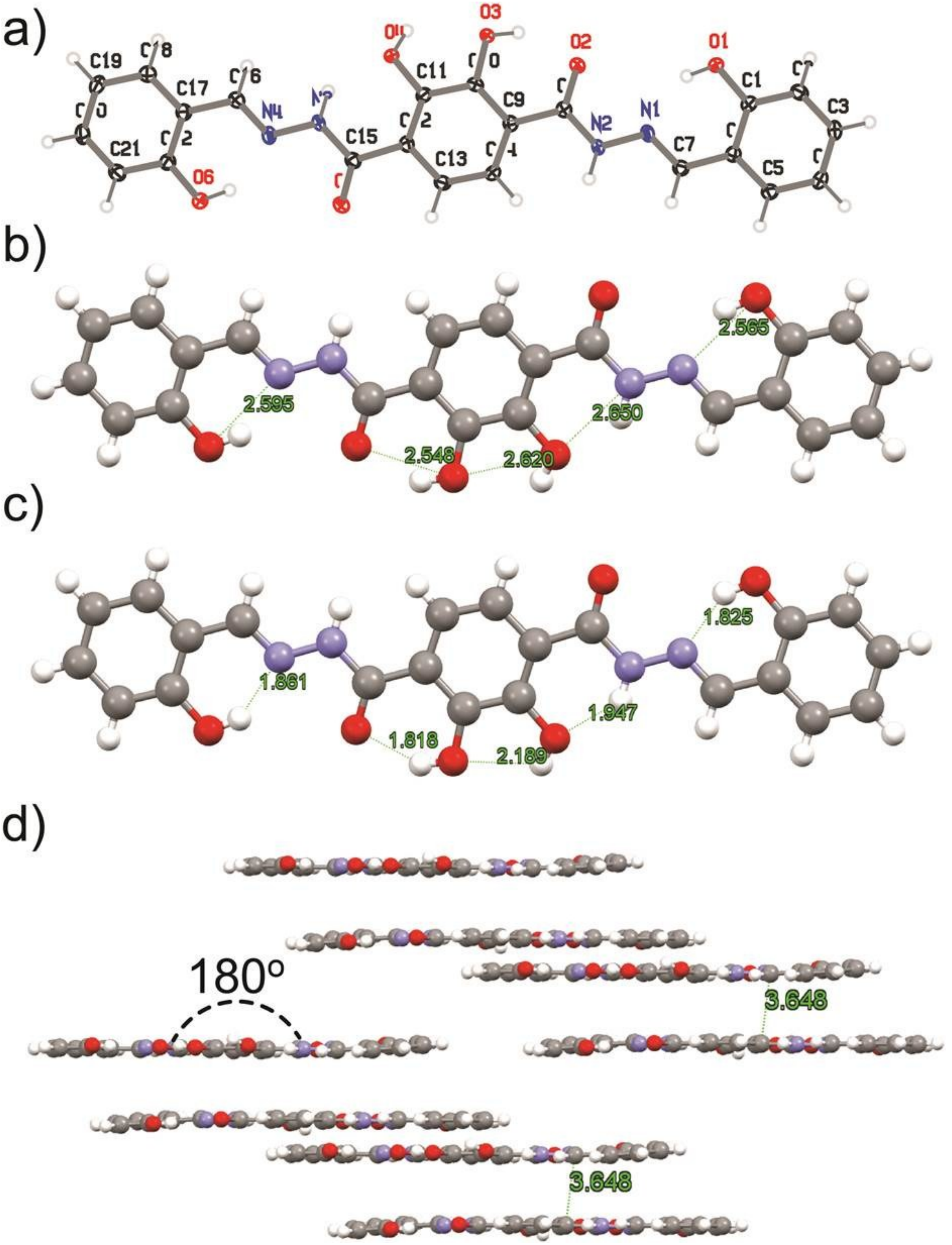

Figure S9. a) ORTEP diagram of Sd-2,3-DHTH.[1] b) Distance between hydrogen bond donor acceptor sites in Sd-2,3-DHTH. c) Calculated distance between hydrogen bonds in Sd-2,3-DHTH. d) Three dimensionally stacked packing of the completely planar Sd-2,3-DHTH units with an interlayer distance about 3.64 Å, which is still maintained in the corresponding COF structure of NUS-51.

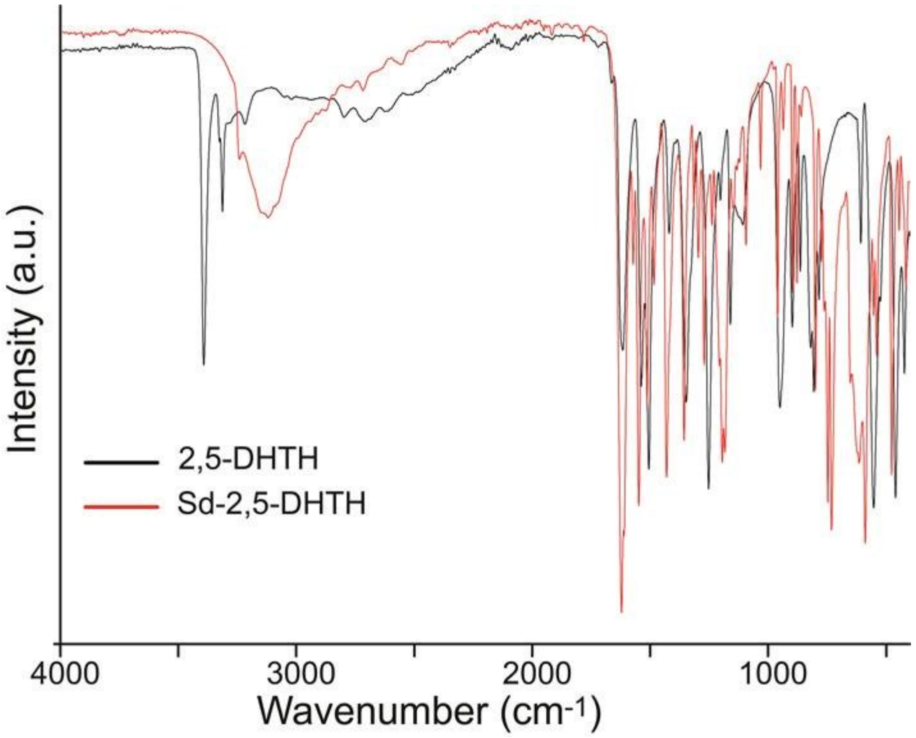

Figure S10. FT-IR comparison between 2,5-DHTH and Sd-2,3-DHTH. The disappearance of the sharp peaks at around 3450 cm^{-1} signifies the consumption of all the amine groups by the formation of hydrazone bond.

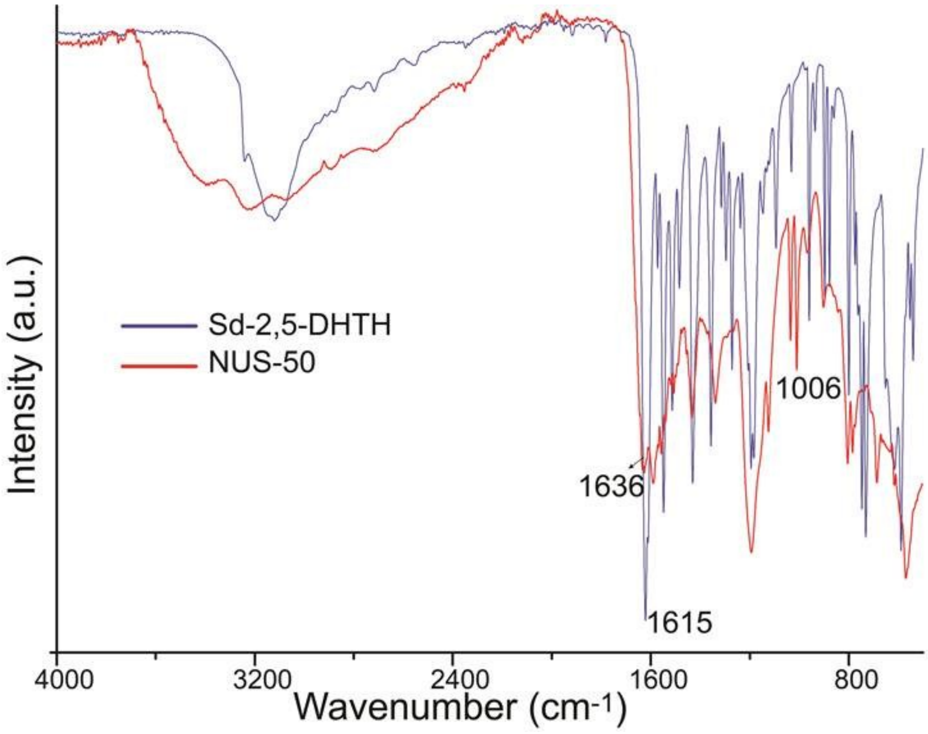

Figure S11. FT-IR comparison between Sd-2,3-DHTH and NUS-50. The appearance of the peak at 1636 cm^{-1} signifies the formation of ketoenamine bond.

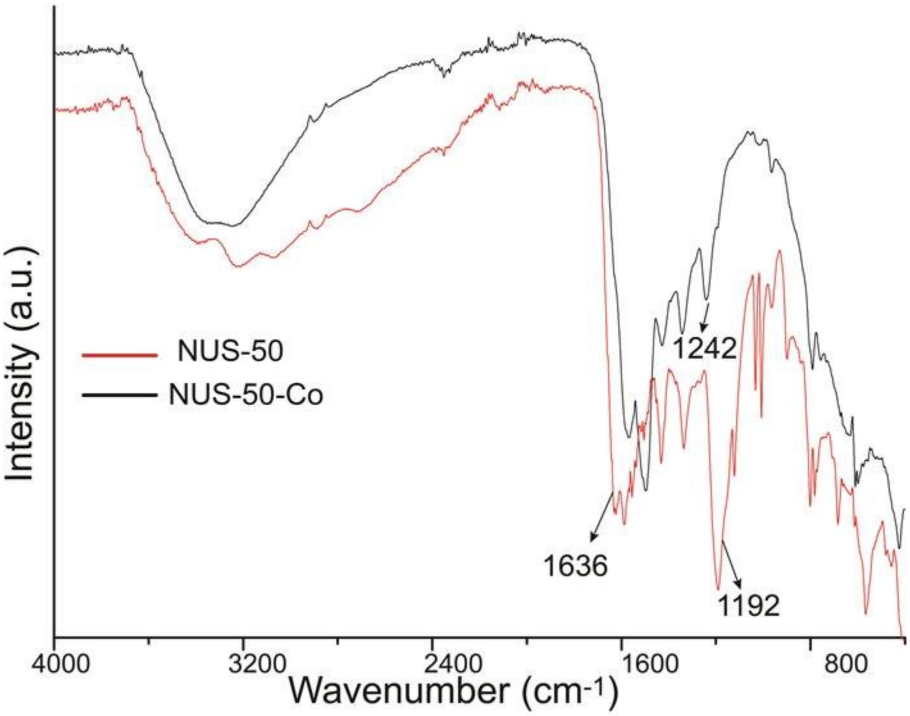

Figure S12. FT-IR comparison between NUS-50 and NUS-50-Co. The broadening of the peaks at 1636 and 1192 cm^{-1} signifies delocalized bonds by coordination with Co^{II}.

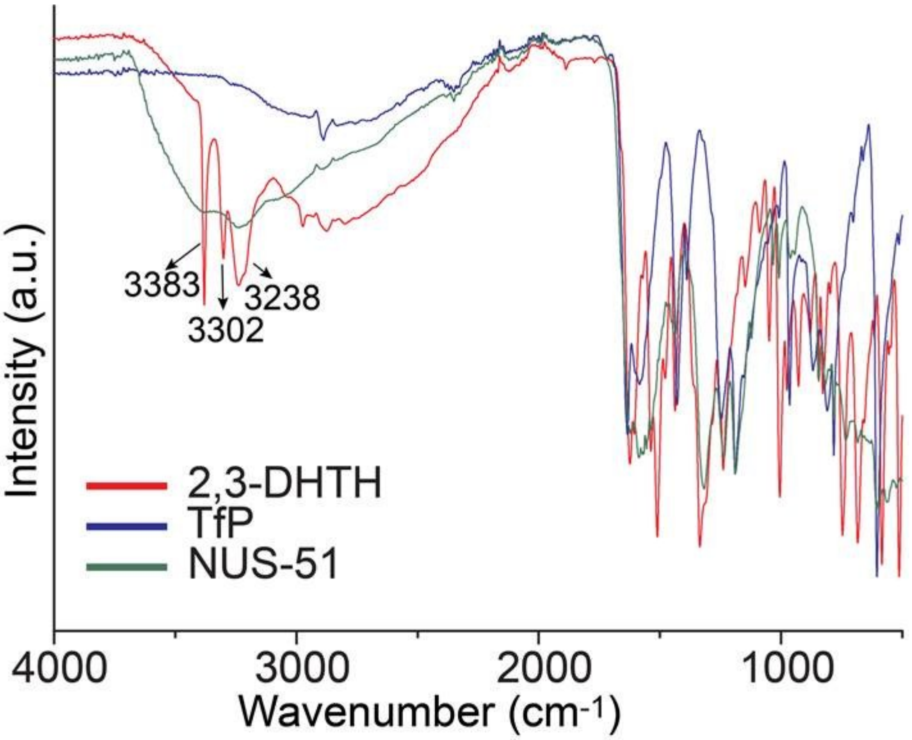

Figure S13. FT-IR comparison between TfP, 2,3-DHTH and NUS-51. The disappearance of the peaks at 3383, 3302 and 3238 cm^{-1} signifies consumption of the free amines of the hydrazide groups.

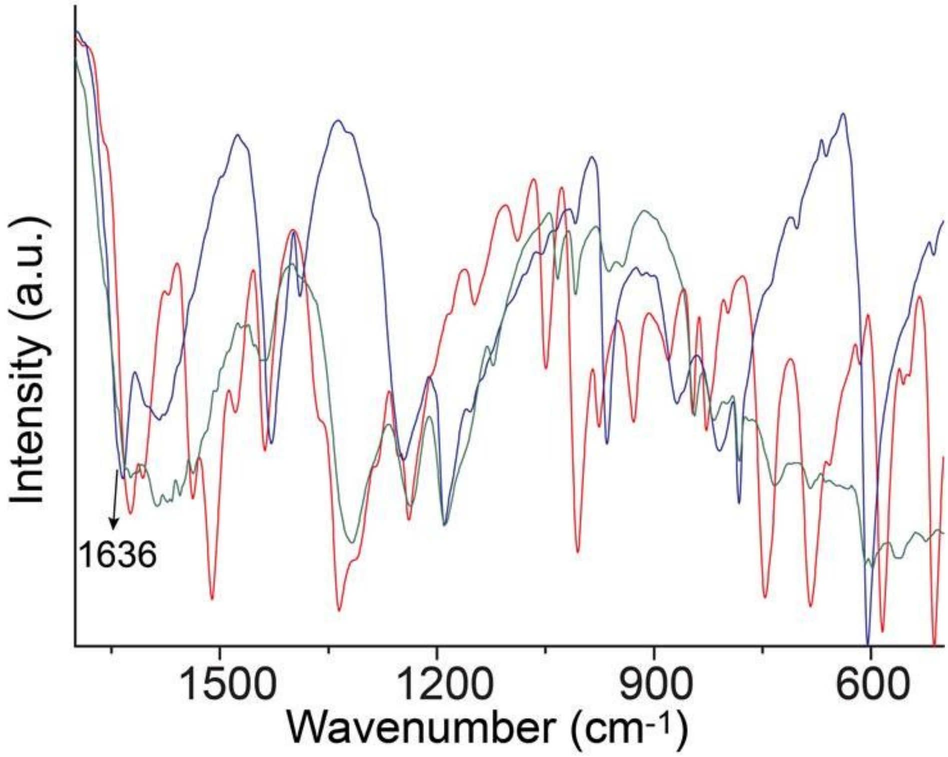

Figure S14. Zoomed-in view (1800-500 cm^{-1}) of the FT-IR comparison between TfP, 2,3-DHTH and NUS-51. The appearance of the new peak at 1636 cm^{-1} signifies the formation of ketoenamine group.

S3: Crystallographic data and graphic images of the COFs

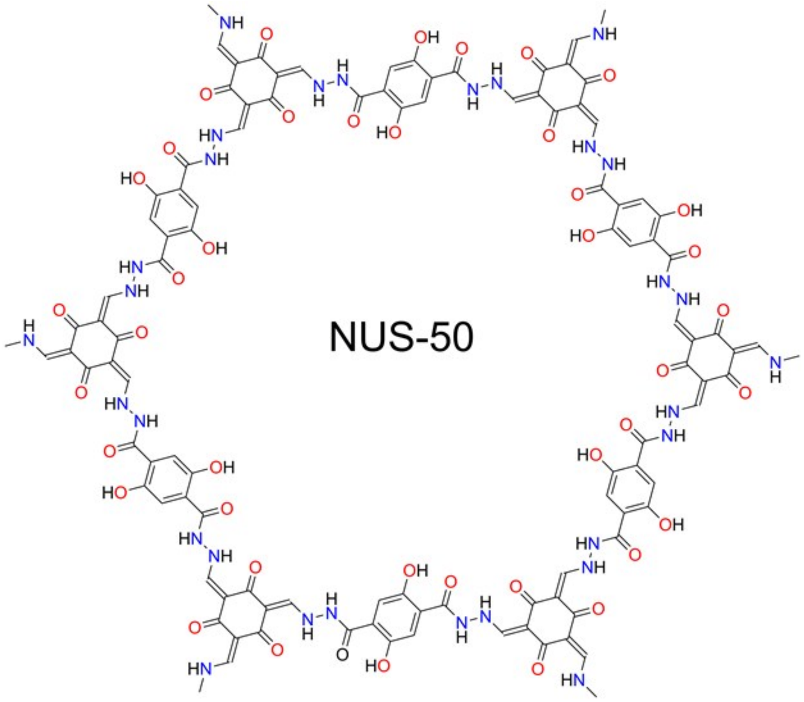

Figure S15. Chemical structure of NUS-50.

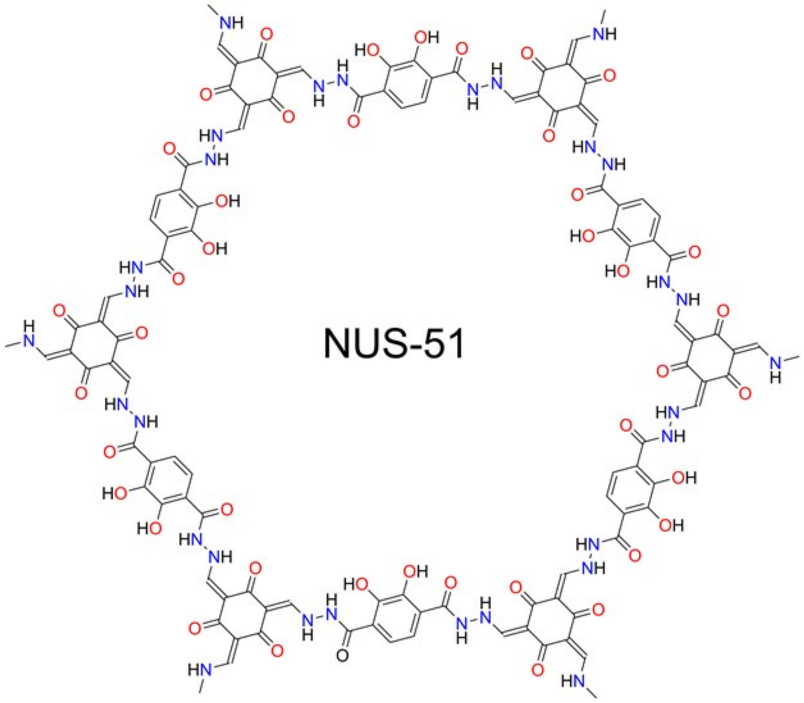

Figure S16. Chemical structure of NUS-51.

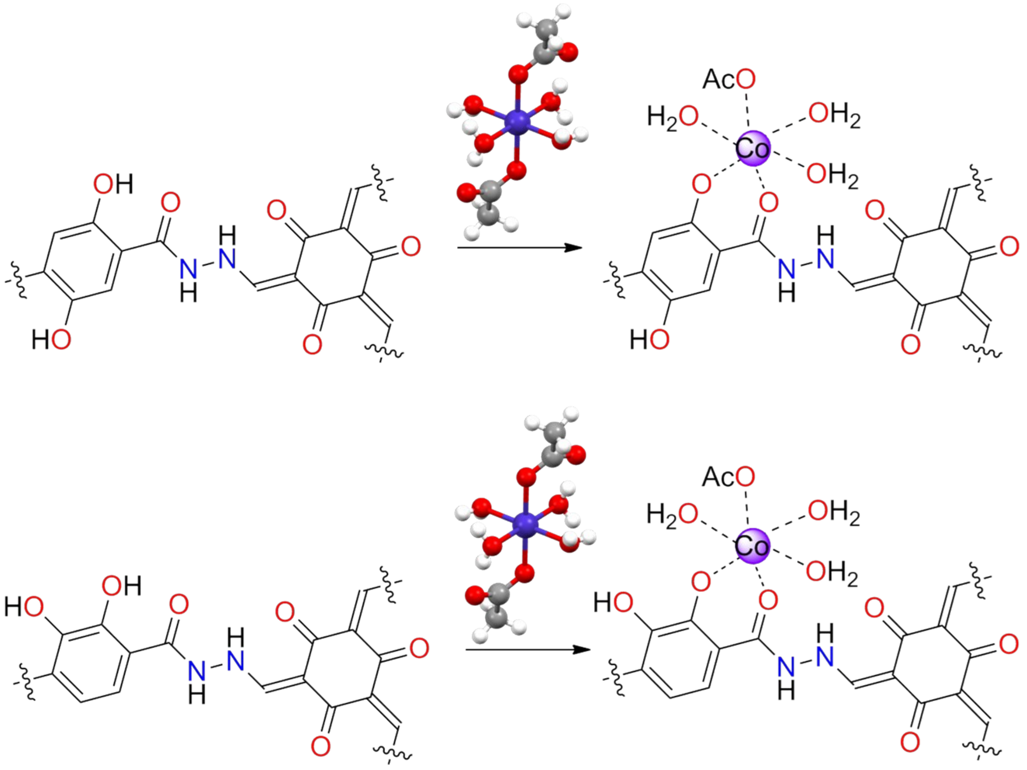

Figure S17. Scheme of Co^{II} loading in NUS-50 (top) and NUS-51 (bottom).

Crystallographic information of modelled NUS-50

Parameter	NUS-50
Empirical formula	$C_7H_5N_2O_3$
F_w	165.13
Stacking method	slipped-AA
Crystal system	Hexagonal
Space group	*P*6/*m*
a [Å]	30.9696
b [Å]	30.9696
c [Å]	3.6000
α [deg]	90.0000
β [deg]	90.0000
γ [deg]	120.0000

Fractional atomic coordinates of NUS-50

Atom site label	*Element*	*Atom site fract x*	*Atom site fract y*	*Atom site fract z*
C1	C	0.29732	0.68484	0
C2	C	0.27884	0.63031	0
C3	C	0.40399	0.63407	0
C6	C	0.41847	0.5205	0
C7	C	0.45951	0.50902	0
C8	C	0.50878	0.54865	0
C9	C	0.54903	0.54019	0

N4	N	0.39268	0.58315	0
N5	N	0.42753	0.56867	0
O10	O	0.37506	0.48711	0
O11	O	0.43231	0.73214	0
O12	O	0.4045	0.42032	0
H13	H	0.44525	0.66348	0
H14	H	0.36394	0.55979	0
H15	H	0.45876	0.59482	0
H16	H	0.51926	0.58737	0
H17	H	0.94518	0.37393	0

Crystallographic information of modelled NUS-51

Parameter	NUS-51
Empirical formula	$C_7H_5N_2O_3$
F_w	165.13
Stacking method	slipped-AA
Crystal system	Hexagonal
Space group	*P*-6
a [Å]	30.9696
b [Å]	30.9696
c [Å]	3.6000
α [deg]	90.0000
β [deg]	90.0000
γ [deg]	120.0000

Fractional atomic coordinates of NUS-51

Atom site label	*Element*	*Atom site fract x*	*Atom site fract y*	*Atom site fract z*
C1	C	0.29732	0.68484	0
C2	C	0.27884	0.63031	0
C3	C	0.40399	0.63407	0
C6	C	0.41847	0.5205	0
C7	C	0.45951	0.50902	0
C8	C	0.50878	0.54865	0
C9	C	0.54903	0.54019	0
C17	C	0.70268	0.31516	0
C18	C	0.72116	0.36969	0
C19	C	0.59601	0.36593	0
C22	C	0.58153	0.4795	0
C23	C	0.54049	0.49098	0
C24	C	0.49122	0.45135	0
C25	C	0.45097	0.45981	0
C22	C	0.58153	0.4795	0
C23	C	0.54049	0.49098	0
C24	C	0.49122	0.45135	0

C25	C	0.45097	0.45981	0
N4	N	0.39268	0.58315	0
N5	N	0.42753	0.56867	0
N20	N	0.60732	0.41685	0
N21	N	0.57247	0.43133	0
O10	O	0.37506	0.48711	0
O11	O	0.43231	0.73214	0
O16	O	0.52237	0.59535	0
O26	O	0.62494	0.51289	0
O27	O	0.56769	0.26786	0
O28	O	0.59742	0.58103	0
H12	H	0.4133	0.42838	0
H13	H	0.44525	0.66348	0
H14	H	0.36394	0.55979	0
H15	H	0.45876	0.59482	0
H29	H	0.55475	0.33652	0
H30	H	0.63606	0.44021	0
H31	H	0.54124	0.40518	0
H32	H	0.48054	0.41259	0
H33	H	0.96163	1.38312	1
H34	H	1.06803	1.44386	1

S4: TGA data

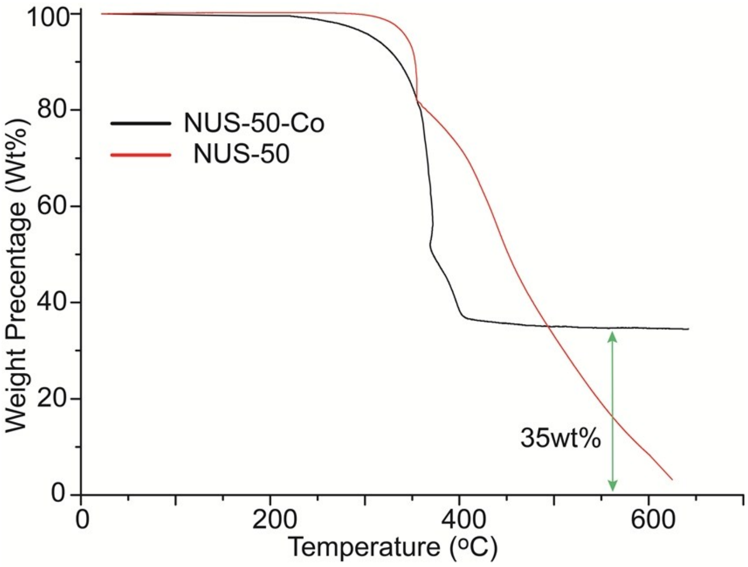

Figure S18. TGA comparison between NUS-50 and NUS-50-Co at an airflow rate of 50 mL min^{-1}. The residual weight above 500 °C in the case of NUS-50-Co arises from cobalt oxide, from which the loading amount of metal ion can be calculated.

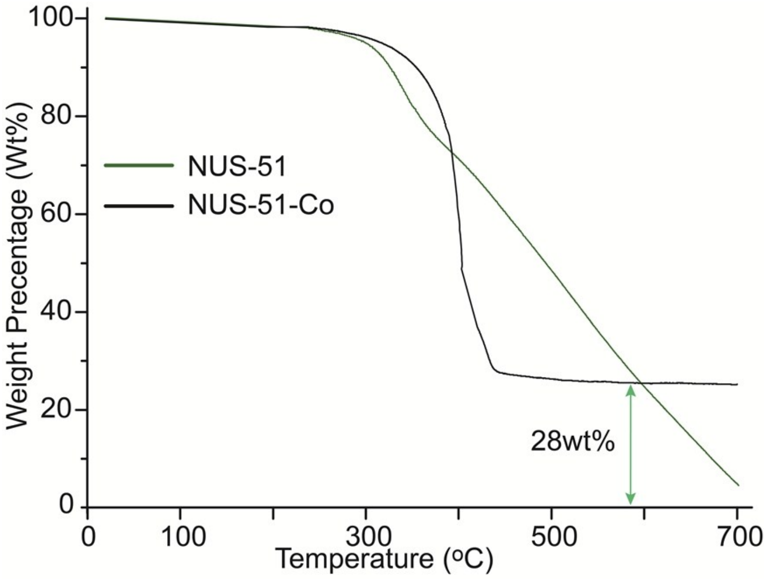

Figure S19. TGA comparison between NUS-51 and NUS-51-Co at an airflow rate of 50 mL min^{-1}. The residual weight above 500 °C in the case of NUS-50-Co arises from cobalt oxide, from which the loading amount of metal ion can be calculated.

S5: XRD data

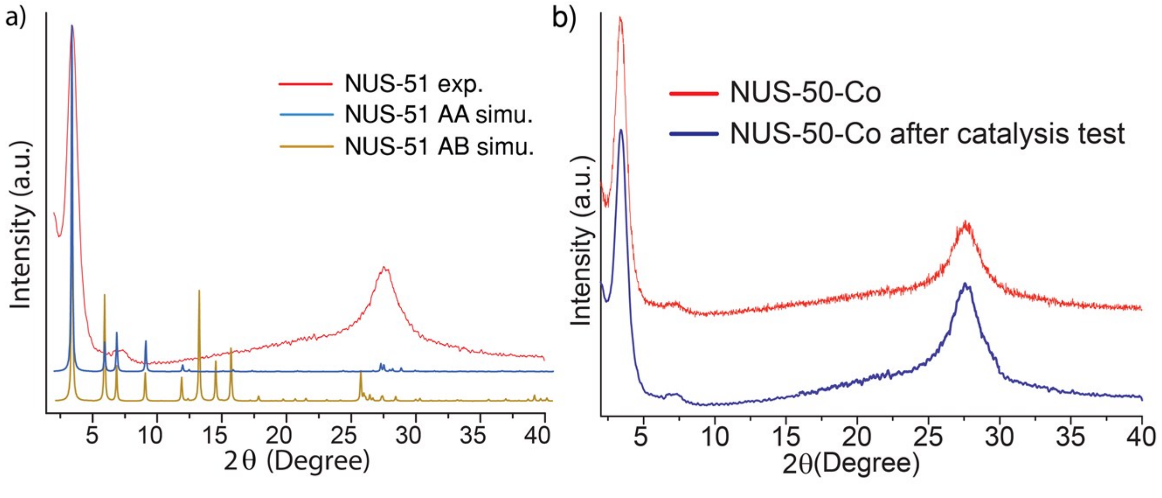

Figure S20. a) PXRD comparison of as-synthesized NUS-51 with eclipsed and staggered crystallographic models. b) PXRD comparison of as-synthesized NUS-50-Co before and after catalysis test.

S6: Scanning electron microscopy (SEM) images

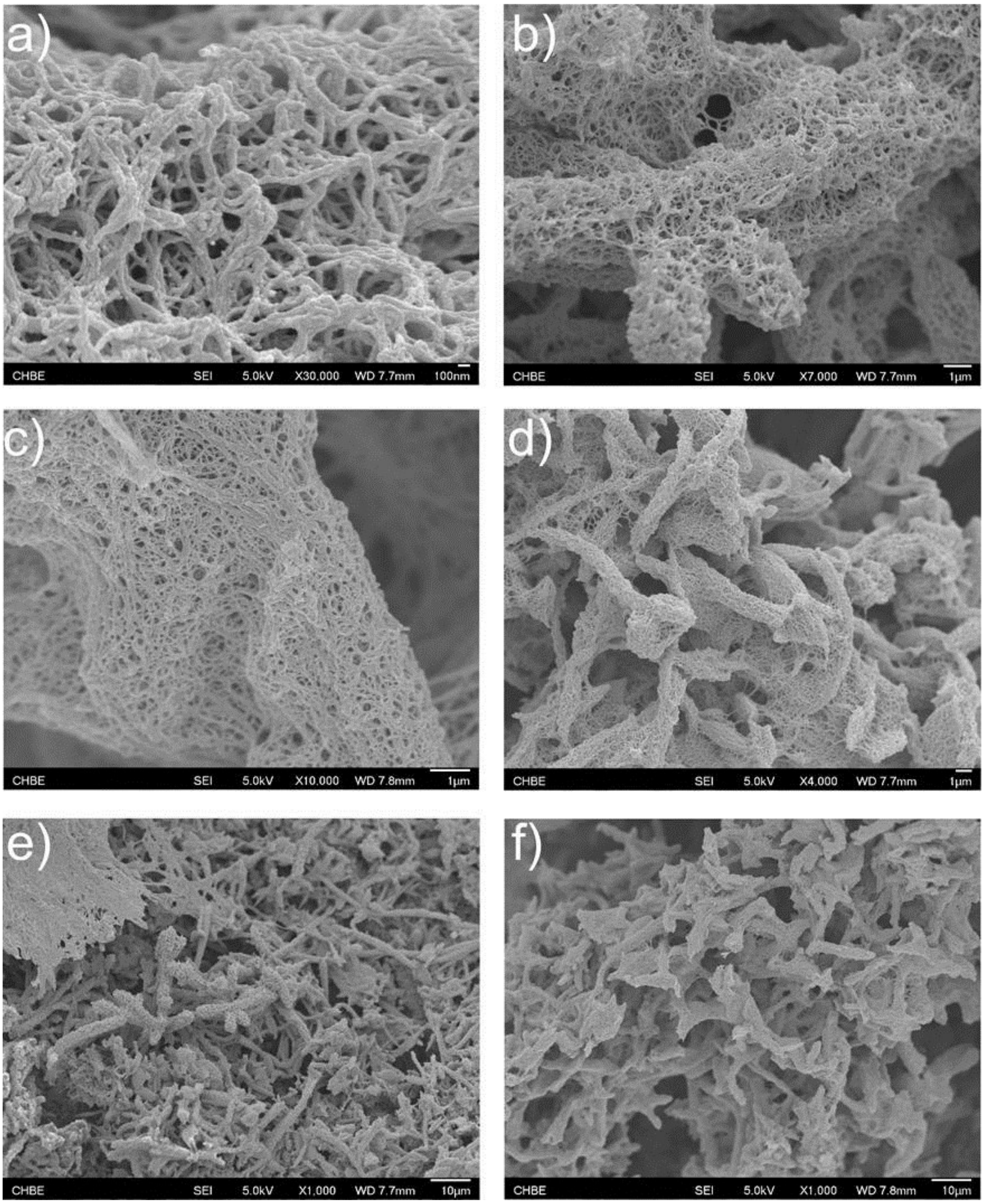

Figure S21. SEM images of a) NUS-50, b) NUS-50-Co, c) NUS-50-Co after catalysis test, d) NUS-51, e) NUS-51-Co, f) NUS-51-Co after catalysis test.

S7: Gas sorption data

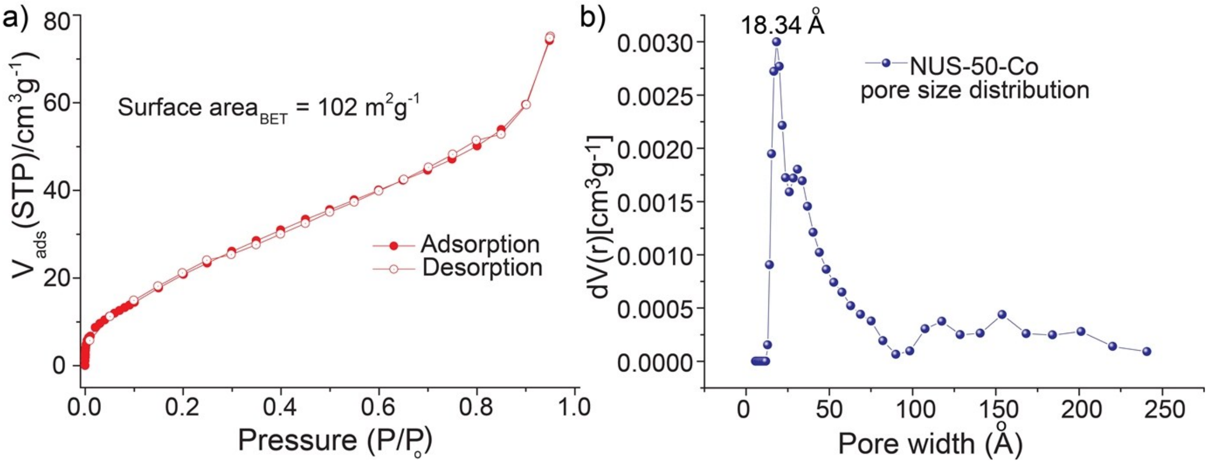

Figure S22. a) Nitrogen sorption isotherm of NUS-50-Co at 77 K, b) pore size distribution of NUS-50-Co.

S8: XPS Spectra of the COFs

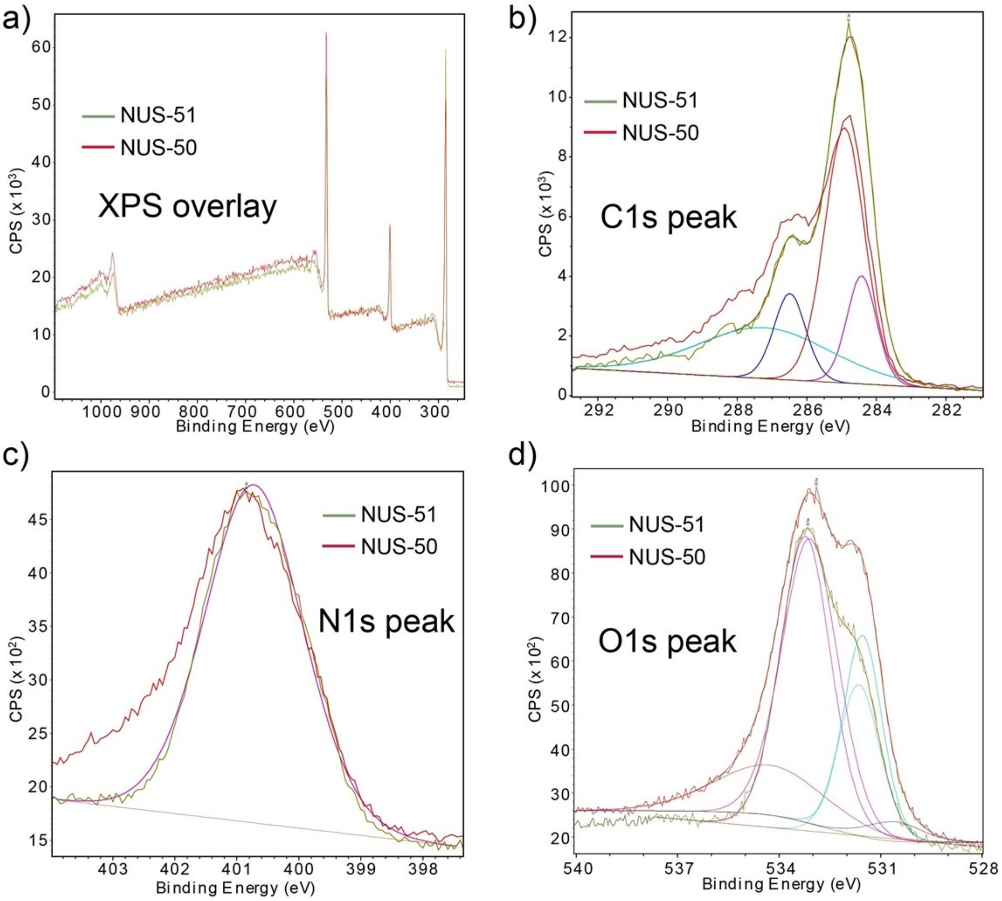

Figure S23. XPS spectra and fit for NUS-50 and NUS-51.

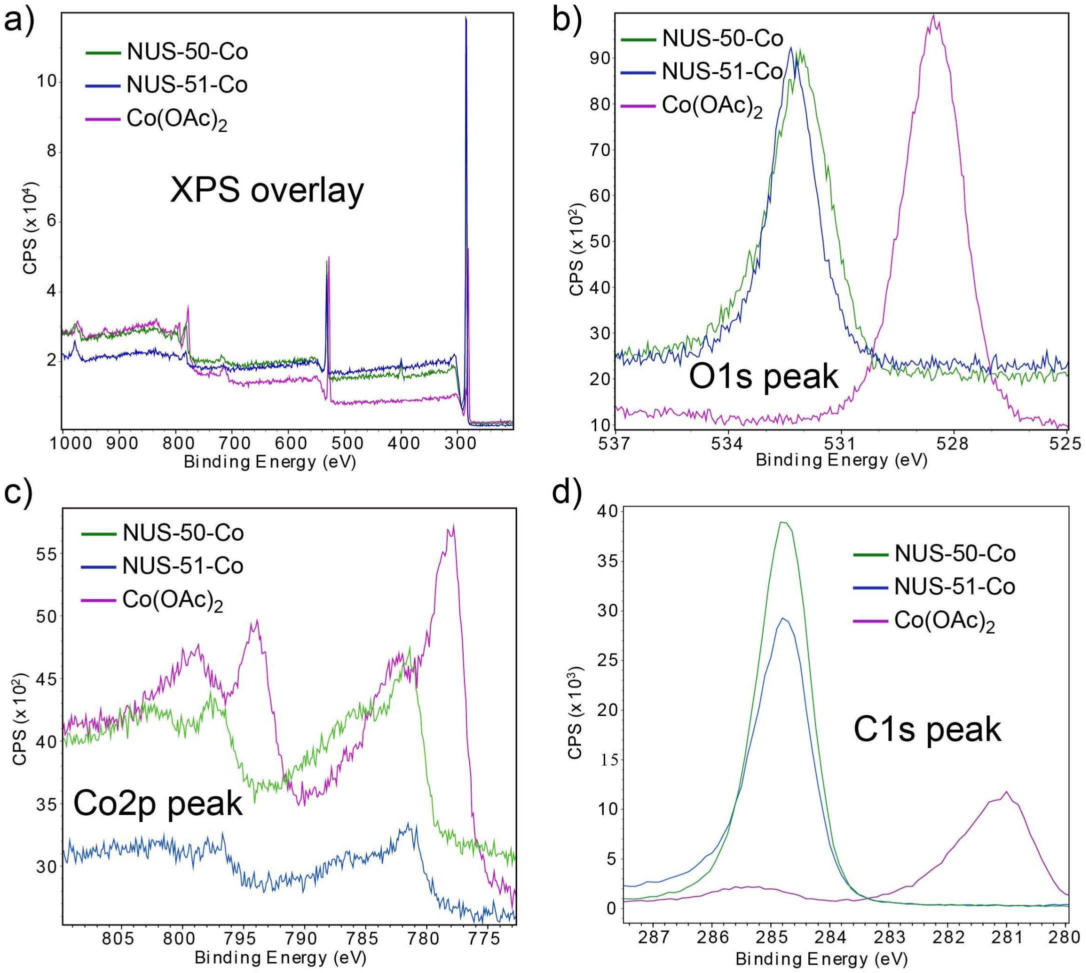

Figure S24. XPS spectra comparison of NUS-50-Co, NUS-51-Co and Co(OAc)$_2$.

S9: Diffuse reflectance spectra (DRS) of the COFs

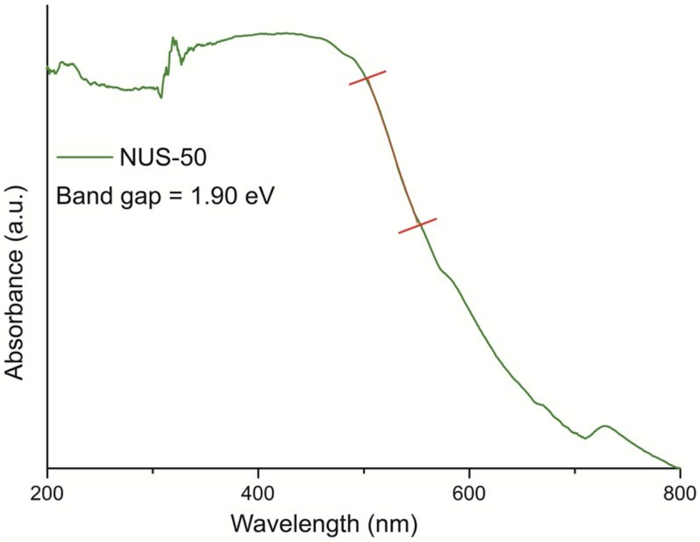

Figure S25. DRS spectrum of NUS-50.

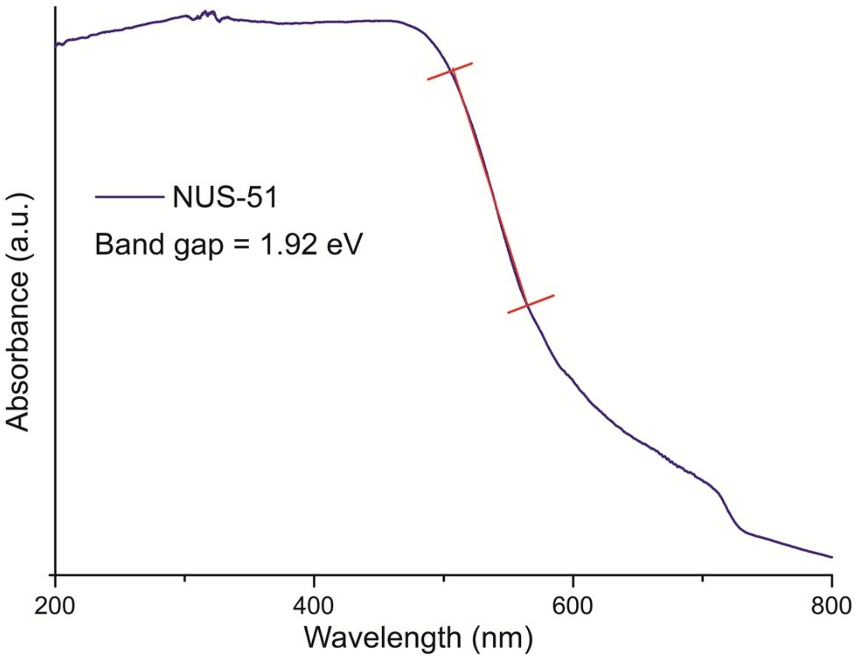

Figure S26. DRS spectrum of NUS-51.

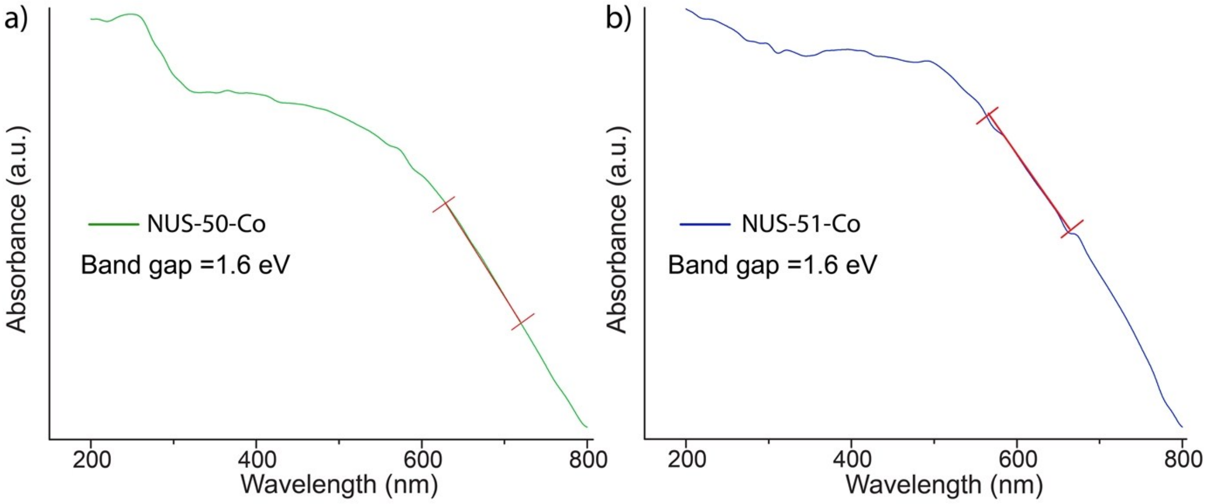

Figure S27. DRS spectrum of a) NUS-50-Co and b) NUS-51-Co.

S10: EXAFS data of the COFs

Co K-edge X-ray absorption fine structure (XAFS) spectra were measured under transmission mode at the XAFCA beamline[2] of Singapore Synchrotron Light Source (SSLS). EXAFS data processing and curve fitting were carried out using Demeter package.[3]

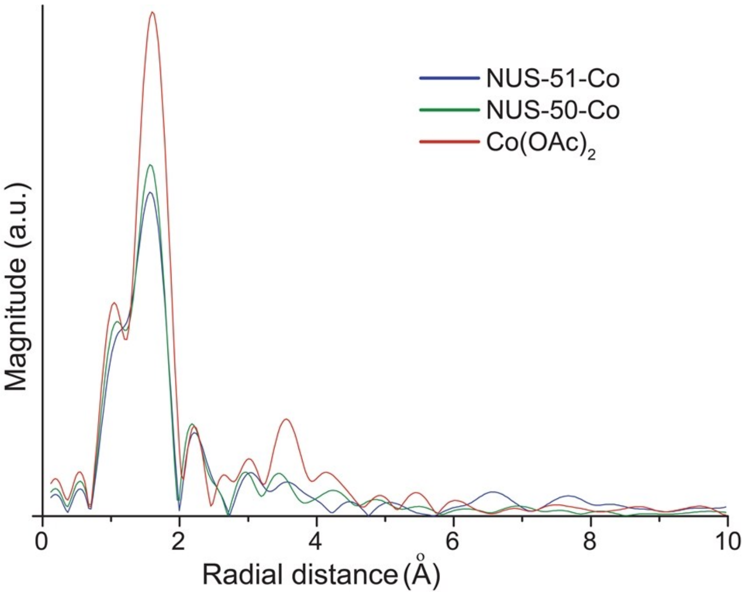

Figure S28. Fourier transformed EXAFS data of NUS-50-Co, NUS-51-Co and Co(OAc)$_2$.

Table for the data fitting parameters

	Bond	***N***	***σ²(Å2)***	***R (Å)***	***R factor***
NUS-51-Co	Co(K)-O	5.7 (0.6)	0.0121 (0.0010)	2.04 (0.02)	0.026
Co(OAc)$_2$	Co(K)-O	6 (0.6)	0.0071 (0.0007)	2.09(0.02)	0.001

S11: Catalysis tests of the COFs

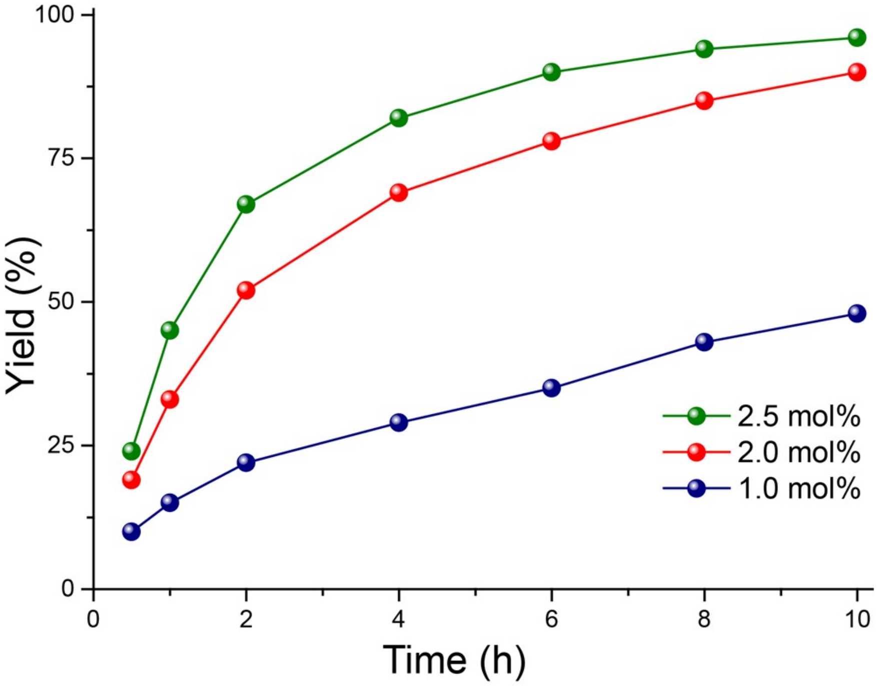

Figure S29. Kinetic profiles for the cyanosilylation of benzaldehyde catalyzed by different amounts of NUS-50-Co.

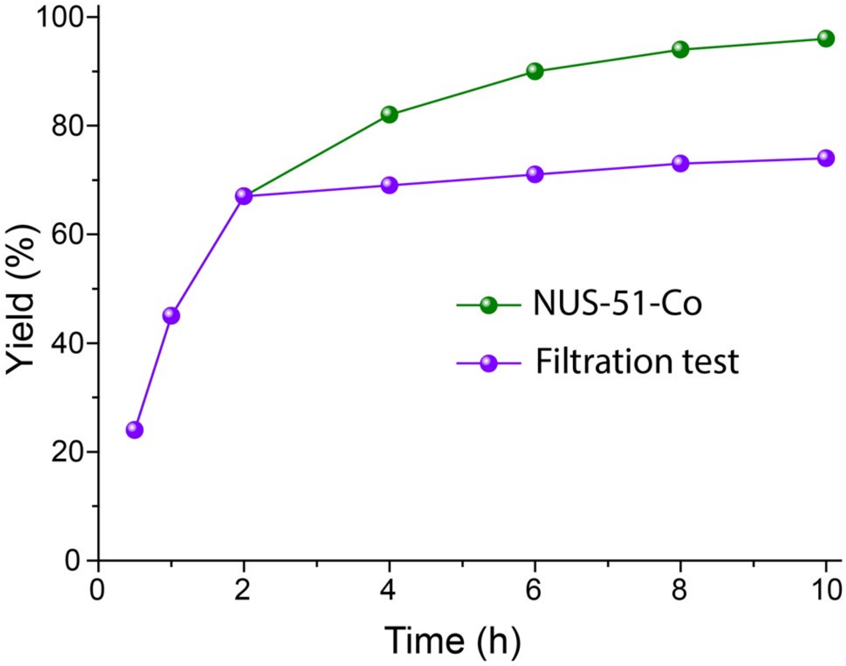

Figure S30. Yields of 2-phenyl-2-trimethylsilyloxyacetonitrile in the cyanosilylation reaction catalyzed by NUS-51-Co (green) and by the filtered solution after 2 h of the reaction (violet).

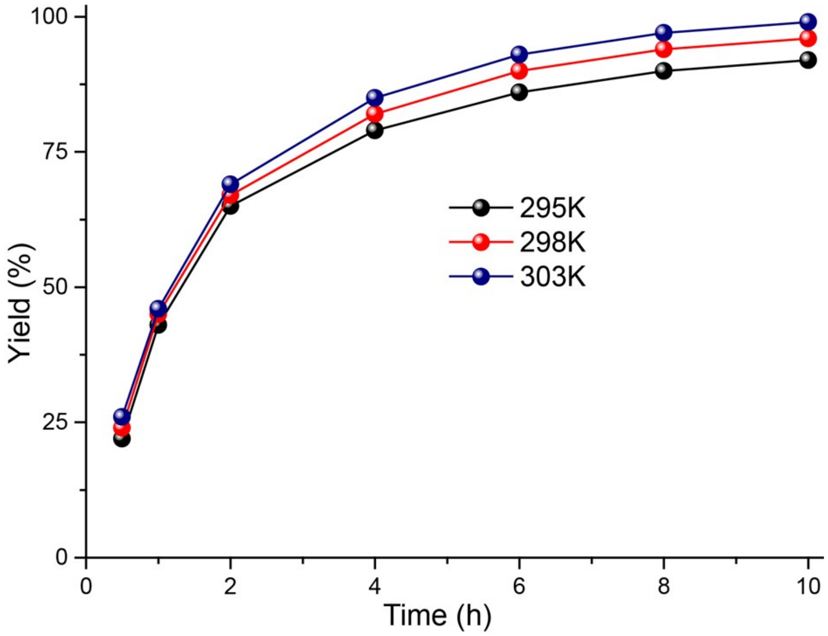

Figure S31. Kinetic profiles for the cyanosilylation of benzaldehyde catalyzed by NUS-50-Co at different temperatures.

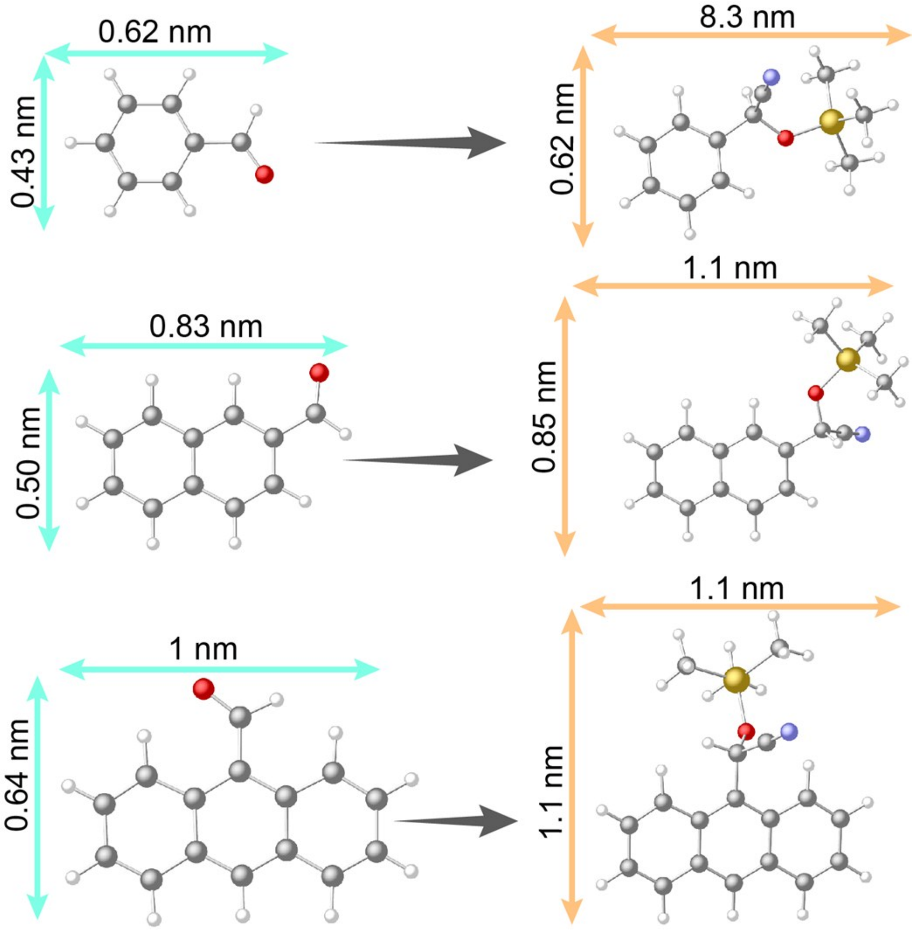

Figure S32. Density functional theory (DFT) optimized structure of reactants and products with their corresponding molecular dimension.

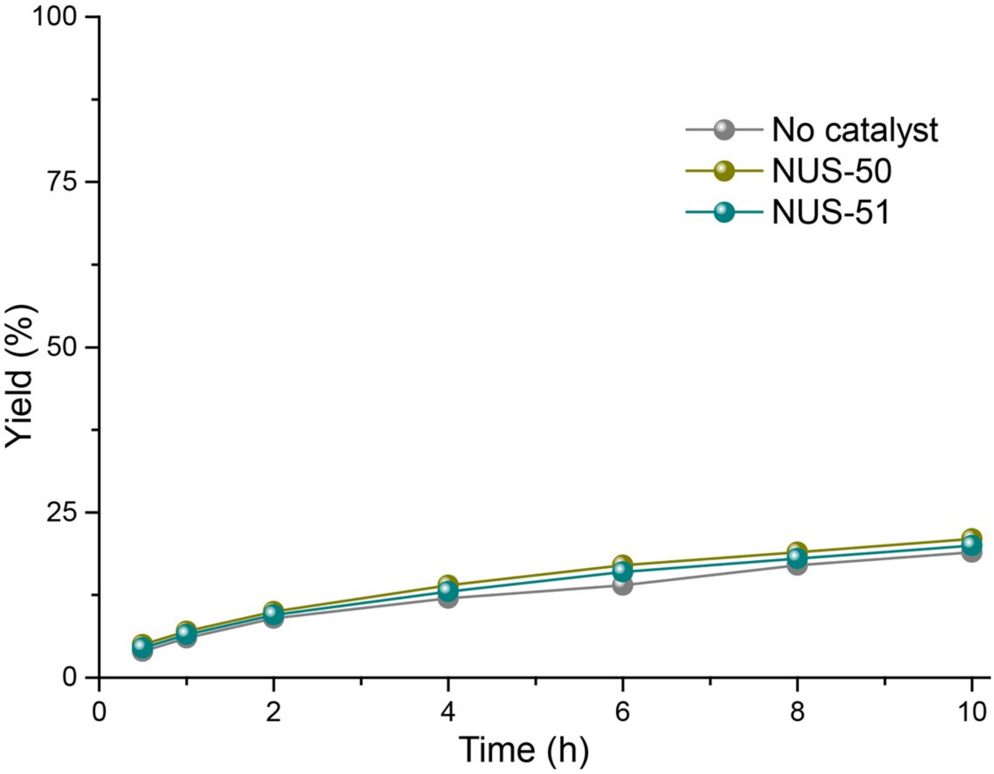

Figure S33. Control experiments without Lewis basic site catalysts.

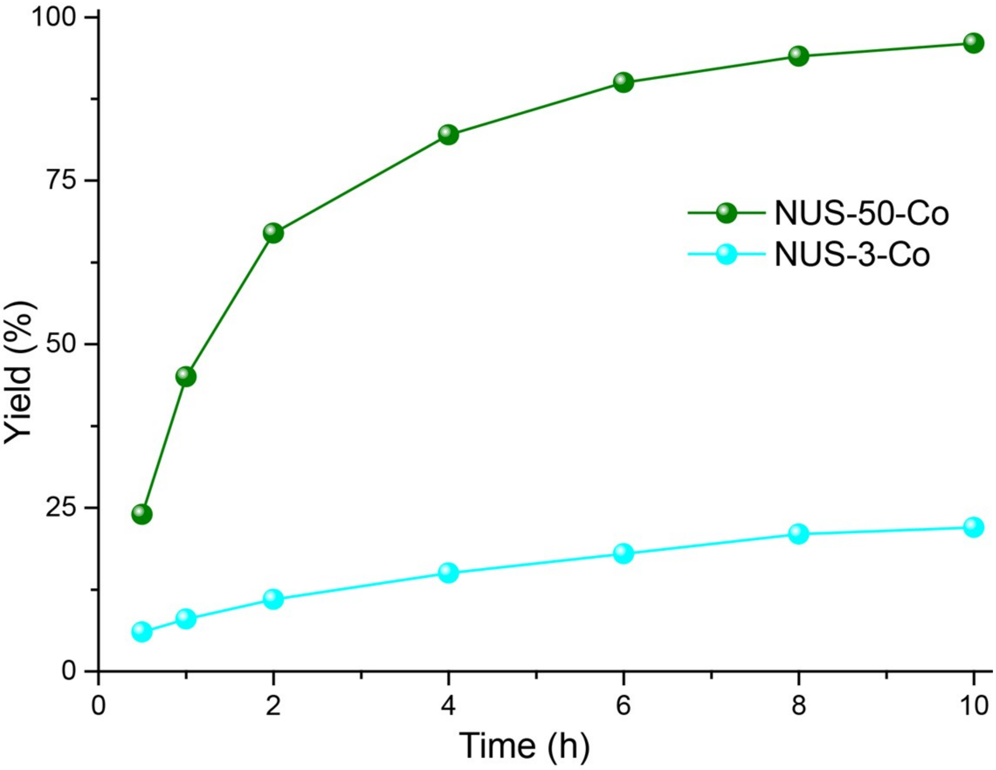

Figure S34. Control experiment with COF having no catalyst loading site.

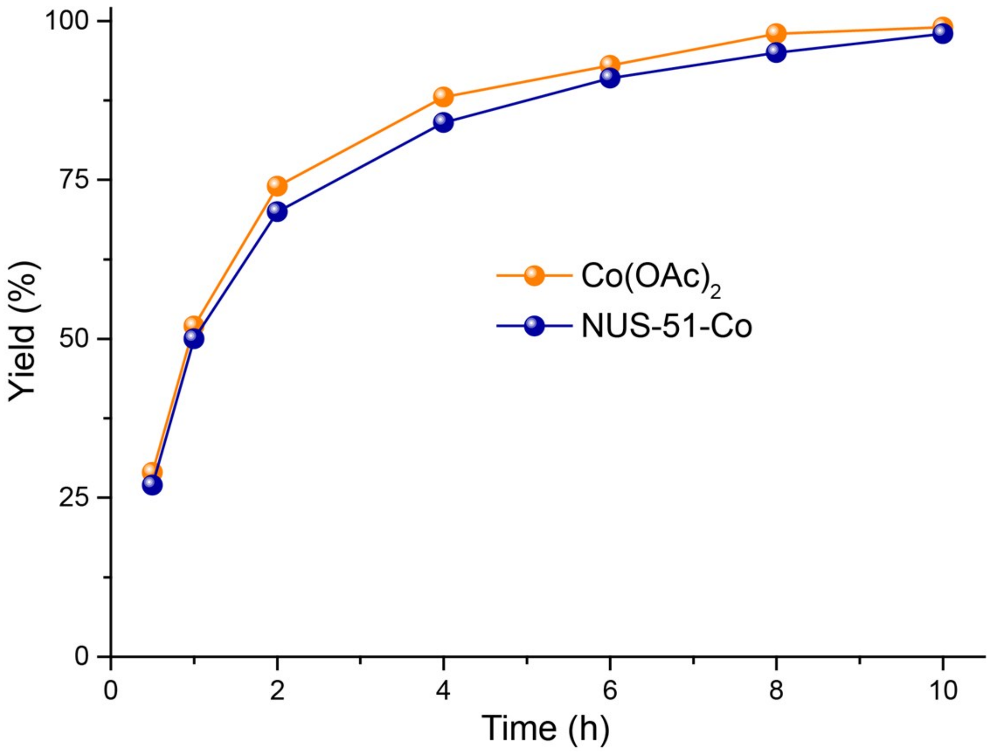

Figure S35. Control experiment with the catalyst precursor and the COF.

Table S1. Catalyst comparison table

Catalyst	Loading (mol%)	Solvent	Temp. (°C)	time (h)	Yield (%)	TON
MIL-101 (Cr)[4]	0.5	heptane	40	3	98	65
$[Mn_3((Mn_4Cl)_3(BTT)_8)_2]_\infty$[5]	11	dichloromethane	25	9	98	8.9
HKUST-1[4]	5	heptane	60	48	55	11
NUS-50-Co *(This work)*	*2.5*	*dichloromethane*	*25*	*10*	*96*	*38*
NUS-51-Co *(This work)*	*2.5*	*dichloromethane*	*25*	*10*	*98*	*39*

S12: References

1. L. Farrugia, *J. Appl. Crystallogr.*, 2012, **45**, 849.
2. Y. Du, Y. Zhu, S. Xi, P. Yang, H. O. Moser, M. B. H. Breese and A. Borgna, *J. Synchrotron Radiat.*, 2015, **22**, 839.
3. B. Ravel and M. Newville, *J. Synchrotron Radiat.*, 2005, **12**, 537.
4. A. Henschel, K. Gedrich, R. Kraehnert and S. Kaskel, *Chem. Commun.*, 2008, 4192.
5. S. Horike, M. Dincă, K. Tamaki and J. R. Long, *J. Am. Chem. Soc.*, 2008, **130**, 5854.